A THEORY OF ELECTRON COLLECTION BY A GRID SPHERE

Juan R. Sanmartin and O. Lopez-Rebollal

Universidad Politecnica de Madrid

28040 Madrid, Spain

ABSTRACT

Use of a spherical grid as electron collector at the anodic end of a tether, as recently proposed, is considered. The standard analysis of space-charge limited current to a solid sphere (with neither magnetic nor plasma-motion effects), which has been shown to best fit TSS1R in-orbit results at very high bias, is used to determine effects from grid transparency on current collected; the analysis is first reformulated in the formalism recently introduced in the two-dimensional analysis of bare-tethers. A discussion of the electric potential created by a spherical grid in vacuum is then carried out; it is shown that each grid-wire collects current well below its maximum OML current, the effective grid transparency being close to its *optical* value. Formulae for the current to a spherical grid, showing the effects of grid transparency, is determined. A fully consistent analysis of electric potential and electron density, outside and inside the grid, is completed.

1 - INTRODUCTION

The TSS1 (1992) and TSS1R (1996) tethers carried insulation all along, and a big solid sphere at the anodic end to collect electrons passively. It was argued as early as 1992 that a tether, bare of insulation for collecting electrons as a giant Langmuir probe in the OML regime, would be a more efficient anode. A detailed comparison of relative performances carried out recently showed the bare tether performing much better than the end-sphere in deorbiting, which fully gauges collection capability, and better to a lesser extent in power generation and thrusting,[1] which are modes of operation less requiring as regards collection. Drag on a big sphere from ram collisions with neutrals is a hindrance, however, for both power generation and thrusting.

To reduce drag, and mass, of a end-sphere collector, it had been proposed to use a grid sphere instead of a solid one; it was suggested that the grid might collect as much current both as the corresponding solid sphere, and as its set of wires performing as “bare tethers” in the OML regime.[2] A detailed study of grid sphere collection requires a previous model of collection by the solid sphere, for which several analyses of TSS1R results concentrated on the non-spherical effects from

the relative plasma motion and the geomagnetic field.[3-7] Actually, best agreement with TSS1R results for the high bias of interest were found[8] using the classical analysis of space-charge limited current to a solid sphere (with neither magnetic nor plasma-motion effects)[9, 10], which we shall also use here. An estimate of an upper bound to the current to a grid sphere has showed a dependence on the optical transparency of the grid.[11]

2 - SPHERICAL SYMMETRY IN GRID COLLECTION

As shown in the next section, desired conditions that lead to collection of current well above the random value, exhibit a region around the sphere where space charge is negligible, the electric potential obeying the Laplace equation. As well known, the electric field generated by a plane metallic grid at given potential in vacuum approaches very rapidly, away from its plane, values corresponding to a metallic plate. The solution to the Laplace equation on the half-space $z > 0$, for an infinite square mesh of side a in the plane $z = 0$, with origin in the center of a mesh and axes parallel to its sides, is symmetric in x, y, and even and periodic in both x and y,

$$\Phi(x, y, z) = \sum_{m=0}^{\infty} \sum_{n=0}^{\infty} \Phi_{mn}(z) \cos\left(\frac{2\pi}{a} mx\right) \cos\left(\frac{2\pi}{a} ny\right), \qquad (1)$$

$$\Phi_{mn} \propto \exp\left(-\frac{2\pi}{a}\sqrt{m^2 + n^2}\, z\right), \qquad m + n > 0. \qquad (2)$$

At distance $z = a$ from the plane, the 0-1 and 1-0 terms in the Fourier representation of Eq.(1) decrease by a factor $e^{-2\pi} \approx 0.002$, $m + n > 1$ terms decreasing faster. The potential is thus rapidly approximated by the term Φ_{00}, which satisfies the equation $d^2\Phi_{00}/dz^2 = 0$, yielding a constant electric field.

Although a spherical grid cannot be made of equal meshes, and the decay away from the grid surface is not exponential, results are quite similar. For a typical mesh side a small enough compared with the radius R the electric potential will be nearly spherically symmetric at a radius $r = R + a$, where the grid surface appears nearly planar. Consider a grid made of $n >> 1$ *meridians* (half-circles) regularly spaced at *longitude* angle $\Delta\phi = 2\pi/n$, and $q \approx n$ *parallels* placed for simplicity at the colatitudes that are roots of the equation $P_q(\cos\theta) = 0$, where P_q is the Legendre polynomial. For $r > R$, the solution to the Laplace equation can be written as

$$\Phi(r, \theta, \phi) = \sum_{m = 0, n, 2n, \ldots} \sum_{l = m}^{\infty} \frac{\Phi_{lm} R^{l+1}}{r^{l+1}} P_l^m(\cos\theta) \cos m\phi \qquad (3)$$

where $P_l^m(\cos\theta)$ is an associated Legendre function, and we used the fact that Φ must be here periodic in ϕ with period $2\pi/n$.

The $l = m = n$ term in (3) has the slower decrease with r among $m \neq 0$ terms. Let a be distance between *meridians* at the *equator*, $n\,a = 2\pi R$, or $a/R = 2\pi/n << 1$. From $r = R$ to $r = R + a$, that term decreases as fast as the $m + n = 1$ term in (1),

$$\left(\frac{R}{R + a}\right)^{n+1} = \left(1 + \frac{2\pi}{n}\right)^{-(n+1)} \approx \exp(-2\pi). \qquad (4)$$

As regards the $m = 0$ terms, the average of Φ at the spherical grid surface in (22), over the full range $0 < \phi < 2\pi$,

$$\int_0^{2\pi} \Phi(R,\theta,\phi)\frac{d\phi}{2\pi} = \sum_{l=0}^{\infty} \Phi_{l0}\, P_l(\cos\theta), \qquad (5)$$

at the *colatitude* of each *parallell* wire, must be the common potential of all grid wires, Φ_P. The sum in (5) can then be reduced to two terms ($\Phi_{l0} = 0$, for $l \neq 0, q$), the average in (5) indeed taking the common value $\Phi_{00} = \Phi_P$ at all *parallel* wires. The $m = 0$ sum in (3) is then just

$$\sum_{l=0}^{\infty} \frac{\Phi_{l0}\, R^{l+1}}{r^{l+1}} P_l(\cos\theta) \;\Rightarrow\; \frac{\Phi_P\, R}{r} + \frac{\Phi_{q0}\, R^{q+1}}{r^{q+1}} P_q(\cos\theta), \qquad (6)$$

the last term decreasing from $r = R$ to $r = R + a$, by a factor about $exp(- 2\pi q/n)$.

Clearly, radial density and potential profiles can be determined assuming full spherical symmetry, with local grid effects only occurring in a narrow region around the sphere. Note that OML collection by the grid wires as suggested[2] would require electrons to move as in a central field of each wire, far from other wires, throughout their motion from infinity; this is clearly not the case, incoming electrons approaching near-radially except in a thin radial range, where the potential hardly changes.

As shown in the next section, however, grid transparency will have a fundamental effect on gross features of the solution, particularly on the current collected. The *optical* transparency α for a "characteristic square" mesh, with distance between centers of closest mesh wires $a << R$, each wire having diameter $d_w << a$, would then be $\alpha = (1- d_w/a)^2$.

3 - MODIFIED OUTER SOLUTION AND LAW FOR CURRENT

The formalism developed for current collection by a bare tether or a cylindrical probe[12, 13] when extended to a spherical collector yields the following expressions for density and inward current of the attracted species,[14]

$$N_e(r) = N_\infty \int_o^\infty \frac{dE}{kT} \frac{\exp(-E/kT)}{\sqrt{\pi}\sqrt{2m_e r^2 kT}} \times \int \frac{dJ^2/2}{\sqrt{J_r^2(E) - J^2}}, \qquad (7)$$

$$I(r) = 4\pi r^2 e N_e u_r = 4\pi r^2 e N_\infty \int_0^\infty \frac{d\varepsilon\; e^{-\varepsilon}}{\sqrt{\pi}\sqrt{2m_e r^2 kT}} \times \int \frac{\pm\, dJ^2}{2m_e r}, \qquad (8)$$

where

$$E \equiv \tfrac{1}{2} m_e(v_r^2 + v_\perp^2) - e\Phi(r) \sim kT, \qquad J \equiv m_e r v_\perp, \qquad (9a, b)$$

$$m_e r v_r = \pm\sqrt{J_r^2(E) - J^2}, \qquad J_r^2(E) \equiv 2m_e r^2 \left[E + e\Phi(r)\right]. \qquad (10a, b)$$

In Eq.(8) the + sign corresponds to negative v_r.

Clearly, from Eq.(10a), only incoming electrons having $J < J_r^*(E)$, with

$$J_r^*(E) \equiv \min imum \left[J_{r'}(E), \quad r \le r' < \infty \right], \tag{11}$$

will reach any given r and contribute to both (7) and (8). Also, all incoming electrons in the range $J_R^*(E) < J < J_r^*(E)$ will turn around before reaching the sphere and contribute to both (7) and (8) too. As regards incoming electrons in the range $0 < J^2 < J_R{}^*(E)^2$, which do reach R^+, the grid collects a fraction $(1 - \alpha)$, while a fraction α will appear at R^- moving inwards with kinetic energy about $e\Phi_P$, and will finally be outgoing at R^-, a fraction of them $\alpha\,(1 - \alpha)$ being collected, and a fraction $\alpha \times \alpha$ appearing at R^+ and moving outwards.

In Eq. (8) we thus have

$$\int dJ^2 \;\Rightarrow\; \int_0^{J_r{}^{*2}} dJ^2 - \int_{J_R{}^{*2}}^{J_r{}^{*2}} dJ^2 - \alpha^2 \int_0^{J_R{}^{*2}} dJ^2 = (1 - \alpha^2)\, J_R{}^{*2}, \tag{12}$$

making I in (8) r-independent as it should. Introducing the random current, $I_{th} = 4\pi R^2 j_{th}$ with $j_{th} = eN_\infty \sqrt{kT / 2\pi m_e}$, we finally find

$$F \equiv \frac{I}{I_{th}} = (1 - \alpha^2) \times \int_0^\infty \frac{d\varepsilon\, e^{-\varepsilon}\, J_R{}^{*2}(\varepsilon)}{2 m_e R^2 kT}. \tag{13}$$

Similarly, in Eq.(7) we have

$$\int \frac{dJ^2}{\sqrt{J_r^2 - J^2}} \;\Rightarrow\; \int_0^{J_r{}^{*2}} \frac{dJ^2}{\sqrt{J_r^2 - J^2}} + \int_{J_R{}^{*2}}^{J_r{}^{*2}} \frac{dJ^2}{\sqrt{J_r^2 - J^2}} + \alpha^2 \times \int_0^{J_R{}^{*2}} \frac{dJ^2}{\sqrt{J_r^2 - J^2}}. \tag{14}$$

The OML current law would hold in case $J_R{}^{*2}(E) \equiv J_R{}^2(E) \equiv 2\, m_e R^2\, (E + e\Phi_P)$, yielding the known result (for the solid sphere, which has $\alpha = 0$), $I / I_{th} = 1 + e\Phi_P / kT \approx e\Phi_P / kT$. The case here of interest, however, corresponds to a large ratio $e\Phi_P / kT$ and a small Debye length $\lambda_D << R$, leading to

$$I/I_{th} << e\Phi_P/kT \quad \Rightarrow \quad J_R{}^{*2}(E) << J_R{}^2(E). \tag{15}$$

$J_R^*(E)$ arises from an envelope in the family of straight lines $J^2 = J_r{}^2(E)$ in the E-J^2 plane, with r as parameter,[12, 14] which sets up at a sheath front where $r^2\Phi(r)$ increases rapidly (Figure 1), yielding $J_R^*(E) \approx J_{env}(E)$. The r-range of lines determining the envelope is narrow and may be characterized by a sheath radius r_{sh}. Inside the sheath, $e\Phi/kT$ increases rapidly with decreasing r, allowing to write $J_r(E) >> J_r^*(E) = J_R^*(E) \approx J_{env}(E)$, with $J_r{}^2(E) \approx 2m_e r^2 e\Phi(r)$. Using (14) with the middle integral now vanishing, in Eq.(7), we find

$$n_e(r) = (1 + \alpha^2) \times \int_0^\infty \frac{d\varepsilon\, e^{-\varepsilon}}{\sqrt{\pi}} \frac{J_r - \sqrt{J_r{}^2 - J_R{}^{*2}}}{\sqrt{2 m_e r^2 kT}}. \tag{16}$$

Since J_R^*/J_r is small, (16) becomes

$$\frac{N_e(r)}{N_\infty} \equiv n_e \approx (1+\alpha^2)\times\frac{1}{2\sqrt{\pi}}\sqrt{\frac{kT}{e\Phi(r)}}\int_0^\infty \frac{d\varepsilon\, e^{-\varepsilon} J_R^{*2}}{2m_e r^2 kT} \qquad (17)$$

or, using (13),

$$n_e(r) \approx \frac{1+\alpha^2}{1-\alpha^2}\times\frac{1}{2\sqrt{\pi}}\frac{R^2}{r^2}\sqrt{\frac{kT}{e\Phi(r)}}\times F\,. \qquad (18)$$

Poisson's equation within the sheath, with $\lambda_D^2 \equiv kT\varepsilon_0/e^2N_\infty$,

$$\frac{1}{r^2}\frac{d}{dr}r^2\frac{d\Phi}{dr} \approx \frac{eN_e}{\varepsilon_0} \qquad \Rightarrow \qquad \frac{d}{dr}r^2\frac{d}{dr}\frac{e\Phi}{kT} \approx \frac{r^2}{\lambda_D^2}n_e\,, \qquad (19a, b)$$

reads, using Eq.(18)

$$\frac{d}{dr}r^2\frac{d}{dr}\frac{e\Phi}{kT} = \frac{1+\alpha^2}{1-\alpha^2}\frac{R^2}{\lambda_D^2}\frac{1}{2\sqrt{\pi}}\sqrt{\frac{kT}{e\Phi(r)}}\,F \qquad (20)$$

$$\Rightarrow \qquad \frac{d}{d\tilde{r}}\tilde{r}^2\frac{dg}{d\tilde{r}} = \frac{1}{\sqrt{g}}\,, \qquad (21)$$

where we defined

$$\tilde{r} \equiv r/r_{sh}\,, \qquad g \equiv \frac{e\Phi}{kT}\times\left(\frac{\lambda_D}{R}\right)^{4/3}\frac{(4\pi)^{1/3}}{F^{2/3}}\times\left(\frac{1-\alpha^2}{1+\alpha^2}\right)^{2/3}. \qquad (22a, b)$$

The solution to the parameter-free Eq.(21) is uniquely defined by a single boundary condition, $g \to 0$, with g formally vanishing as

$$g \approx \left[3(\tilde{r}-1)/2\right]^{4/3}$$

as $\tilde{r} \to 1$, to match behavior of the potential at the front.[10] Using $\Phi = \Phi_P$ in (22b) to determine $g(\tilde{r})$ at $\tilde{r} = R/r_{sh}$ gives

$$g\left(\frac{R}{r_{sh}}\right) = Y\times\frac{(4\pi)^{1/3}}{F^{2/3}}\times\left(\frac{1-\alpha^2}{1+\alpha^2}\right)^{2/3}, \qquad Y \equiv \frac{e\Phi_P}{kT}\times\left(\frac{\lambda_D}{R}\right)^{4/3}. \qquad (23a, b)$$

From a quasineutral solution in the region outside the sheath one could also write

$$I = c\times 4\pi r_{sh}^2\, j_{th} \qquad \Rightarrow \qquad F \equiv I/I_{th} = c\times r_{sh}^2/R^2. \qquad (24a, b)$$

where c is some constant of order unity obtained, in principle, from an approximate quasineutral analysis.

Equations (23a), (24b) determine the current collected by the grid,

$$\frac{F^{2/3}}{(4\pi)^{1/3}} \times g\left(\sqrt{\frac{c}{F}}\right) = Y\left(\frac{1-\alpha^2}{1+\alpha^2}\right)^{2/3} \qquad (25)$$

$$\Rightarrow \quad \frac{I}{I_{th}} = F\left[Y\left(\frac{1-\alpha^2}{1+\alpha^2}\right)^{2/3}\right], \qquad (26)$$

which recovers the current $I = I_{th} \times F(Y)$ for the solid sphere,[9, 10] as given in figure 3 of Reference 8. For small $\tilde{r}$ (as it holds near the sphere in case F, and thus r_{sh}/R, is large) one finds

$$g(\tilde{r}) \propto 1/\tilde{r} \quad \Rightarrow \quad F \sim Y^{6/7}. \qquad (27)$$

The behavior near the sphere $g \propto 1/\tilde{r}$ corresponds to the space-charge free solution, $\Phi \propto 1/r$, as advanced in Sec.2.

4 - INNER SOLUTION

Inside the sphere, Poisson´s equation (19b) must be solved under boundary conditions $\Phi(R) = \Phi_P$ and $d\Phi/dr = 0$ at $r = 0$. This will require some positive slope at R^- and thus a jump in $d\Phi/dr$, the slope at R^+ being prescribed by the outer solution and negative. Clearly, the slope at the spherical surface in the space between wires must be continuous; a jump occurs just at the wires, due to the appropriate surface charges. These differences, however, will be limited to a narrow layer and can be ignored here, as in the discussion in Sec.2.

Inside the spherical grid surface, where there is no collector and the electron distribution function is even in v_r, current vanishes throughout. Negative and positive v_r contributions add for density, however, yielding in Eq.(7)

$$n_e(r) = \int_0^\infty \frac{d\varepsilon\, e^{-\varepsilon}}{\sqrt{\pi}\sqrt{2m_e r^2 kT}} \times 2\alpha \int_0^{J_r^*} \frac{dJ^2/2}{\sqrt{J_r^2(E) - J^2}} \qquad (28)$$

$$= 2\alpha \int_0^\infty \frac{d\varepsilon\, e^{-\varepsilon}}{\sqrt{\pi}} \frac{J_r(E) - \sqrt{J_r^2(E) - J_r^{*2}(E)}}{\sqrt{2m_e r^2 kT}}. \qquad (29)$$

For some radial range from $r = R^-$ inwards ($r > \hat{r}$ in Figure 1) we will still have $J_r^* = J_R^* < J_r$, with $e\Phi >> kT$ or $J_r^2 \approx 2m_e r^2 e\Phi$, and (29) becomes

$$n_e(r) = \frac{2\alpha}{\sqrt{\pi}} \times \int_0^\infty d\varepsilon\, e^{-\varepsilon} \left[\sqrt{\frac{e\Phi(r)}{kT}} - \sqrt{\frac{e\Phi(r)}{kT} - \frac{{J_R^*}^2}{2m_e r^2 kT}} \right] \tag{30}$$

$$\approx \frac{2\alpha}{\sqrt{\pi}} \times \left[\sqrt{\frac{e\Phi(r)}{kT}} - \sqrt{\frac{e\Phi(r)}{kT} - \frac{R^2}{r^2} \frac{F}{1 - T_{opt}^2}} \right], \tag{31}$$

where, for simplicity, we took an ε-average of $J_R^{*2}(E)$ from Eq.(13),

$$F \equiv \frac{I}{I_{th}} \approx (1 - \alpha^2) \times \frac{< {J_R^*}^2 >}{2m_e R^2 kT}. \tag{32}$$

At $r = \hat{r}$ satisfying

$$J_{\hat{r}}^2 \approx 2m_e \hat{r}^2 e\Phi(\hat{r}) = < {J_R^*}^2 > = 2m_e R^2 kT \times \frac{F}{1 - \alpha^2} \tag{33}$$

Eq.(31) reduces to

$$n_e(\hat{r}) = \frac{2\alpha}{\sqrt{\pi}} \sqrt{\frac{e\Phi(\hat{r})}{kT}}. \tag{34}$$

For $r < \hat{r}$, we have $J_r^* = J_r$ and Eq.(29) yields

$$n_e(r) = \frac{2\alpha}{\sqrt{\pi}} \int_0^\infty d\varepsilon\, e^{-\varepsilon} \sqrt{\varepsilon + \frac{e\Phi(r)}{kT}}$$

$$= \frac{2\alpha}{\sqrt{\pi}} \left[\sqrt{\frac{e\Phi}{kT}} + \frac{\sqrt{\pi}}{2} \exp\left(\frac{e\Phi}{kT}\right) erfc \sqrt{\frac{e\Phi}{kT}} \right] \tag{35}$$

recovering (34) at large $e\Phi(\hat{r})/kT$. Here, *erfc* is the complementary error function, and we now kept $J_r^2(E) = 2m_e r^2 [E + e\Phi(r)]$ in full.

Tentatively assuming $\Phi(0)$ positive, Eq. (31) is used for n_e in the range $\hat{r} < r < R$ and Eq.(35) for $0 < r < \hat{r}$. Note that the density in (35) decreases with radius; there is no spherical convergence effect and, certainly, n_e does not diverge as $r \to 0$. Although electron motion at R^- is near radial, as implied by condition $J_r^* << J_r$, it does cover a finite range $0 < J < J_r^* = J_R^*$ in angular momentum; at $r < \hat{r}$, with $J_r^* = J_r$, there exist electrons having $J = J_r$, i.e. $v_r = 0$. For given values of the three dimensionless numbers, $e\Phi_P/kT$, λ_D/R and α [which also determine values for Y and F in (23b) and (26)], one uses (31) to integrate Eq. (19b) inwards,

starting at $r = R$ with values Φ_P and any particular positive slope $d\Phi/dr$. At the radius satisfying condition (33), one continues integration using Eq. (35) from $r = \hat{r}$ to $r = 0$. One must then just sweep over values of the slope at R to finally select that value satisfying condition $d\Phi/dr = 0$ at $r = 0$.

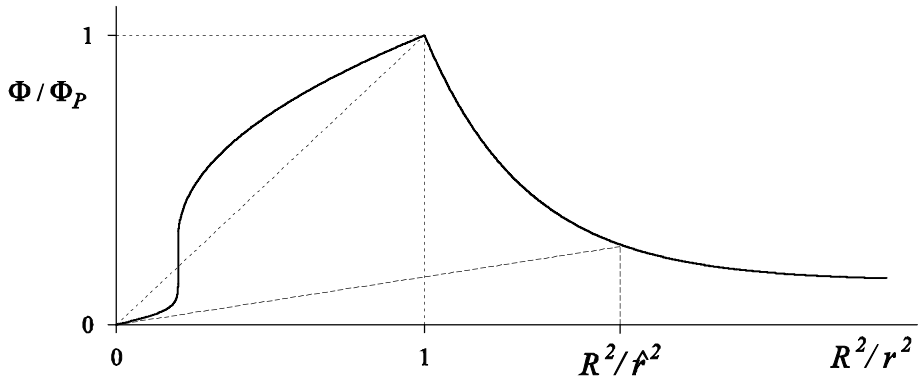

Figure 1 -

5 - CONCLUSIONS

We have discussed a proposal for using a spherical grid in electron collection at the anodic end of a tether, to reduce drag and mass of an end-sphere collector. The standard analysis of space-charge limited current to a solid sphere (with neither magnetic nor plasma-motion effects), which has been shown to best fit TSS1R in-orbit results at very high bias, is used to determine effects from grid transparency on current collected. We first considered the electric potential created by a spherical grid in vacuum, and showed that each grid-wire collects current well below its maximum OML current, the effective grid transparency being very close to its *optical* value.

We then carried out a fully consistent analysis of electric potential and electron density, outside and inside the grid, finally leading to a formula for the current to a spherical grid,

$$\frac{I(\alpha)}{I(\alpha=0)} = \frac{F\left[Y\,(1-\alpha^2)^{2/3}/(1+\alpha^2)^{2/3}\right]}{F(Y)} \qquad (36)$$

[where $I = I_{th} \times F(Y)$ is the current to the solid sphere[9, 10]], showing the effects of grid transparency α. This is to be compared with the estimate in Ref. 11,

$$\frac{I(\alpha)}{I(\alpha=0)} = 1 - \frac{\alpha^2}{2} - \frac{\alpha^4}{2}. \qquad (37)$$

Using (27) for large argument, Eq. (36) yields

$$\frac{I(\alpha)}{I(\alpha=0)} \approx \left(\frac{1-\alpha^2}{1+\alpha^2}\right)^{4/7} \Rightarrow (1-\alpha)^{4/7} \quad \text{for} \quad \alpha \approx 1. \qquad (38)$$

Clearly, the current reduction in (38) relative to the solid sphere would make a bare tether perform much better than a grid sphere in both power generation and thrusting too. On the other hand, the grid sphere [with mass $(1 - \alpha)$ times the mass of the corresponding solid sphere] would have a greater current-to-mass ratio than the solid one. This would also apply to the current-to-drag ratio. In moving from a solid to a grid sphere, drag would be reduced in a factor

$$Drag\ (\alpha) / Drag\ (\alpha = 0) = (1 - \alpha) + \alpha \times b\ (1 - \alpha). \qquad (39)$$

The first term arises from drag at the ram hemisphere, whereas the second term arises from drag at the inner surface of the wake hemisphere. The factor $b < 1$ will depend on how meshes in the first hemisphere are projected into the second one. The result $2(1 - \alpha)$ given in Ref.11 for the drag ratio does not recover the proper limit, 1, for vanishing α, because it ignored the factor α in the second term of (39), which takes into account that the flux of neutrals impacting the inner surface of the wake hemisphere has been reduced in that factor.

6 - BIBLIOGRAPHY

[1] J.R. Sanmartin and E. C. Lorenzini, *IEEE Trans. Pl. Sci.* **34**, 2133 (2006).

[2] N.H. Stone, J.D. Moore, W.R. Clayton and P.A. Gierow, in *Space Technology and Applications International Forum- STAIF* 2002 (ed. M.S. El-Genk, Am. Inst. of Phys.), p.537.

[3] J.G. Laframboise, *J. Geophys. Res.* **102**, 2417 (1997).

[4] D.C. Thompson, C. Bonifazi, B. Gilchrist, S.D. Williams, W.J. Raitt, J.P. Lebreton, W.J. Burke, N.H. Stone and K.H. Wright Jr., *Geophys. Res. Lett.* **25**, 413 (1998).

[5] T.Z. Ma and R.W. Schunk, *Geophys. Res. Lett.* **25**, 737 (1998).

[6] N. Singh and W.C. Leung, *Geophys. Res. Lett.* **25**, 741 (1998).

[7] D.L. Cooke and I. Katz, *Geophys. Res. Lett.* **25**, 753 (1998).

[8] G. Vannaroni, M. Dobrowolny, J.P. Lebreton, E. Melchioni, F. De Venuto, C.C. Harvey, L. Iess, U. Guidoni, C. Bonifazi and F. Mariani, *Geophys. Res. Lett*. **25**, 749 (1998).

[9] Y.L. Alpert, A.V. Gurevich and L.P. Pitaevskii, *Space Physics and Artificial Satellites* (Consult. Bur., New York, 1965), Ch. IX.

[10] S.H. Lam, *Phys. Fluids* **8**, 73 (1965).

[11] G.V. Khazanov, E. Krivorutsky and R.B. Sheldon, *J. Geophys. Res.* **110**, A12304 (2005).

[12] J.R. Sanmartin and R.D. Estes, *Phys. Plasmas* **6**, 1677 (1999); **8**, 4234 (2001)

[13] R.D. Estes and J.R. Sanmartin, *Phys. Plasmas* **7**, 4320 (2000).

[14] J.R. Sanmartin, in *Space Technology Course: Prevention of risks related to Spacecraft Charging*" (ed.J.P. Catani, CEPADUES EDITIONS, 2002), pp. 515-533.

◄ BACK TO SESSION DETAILED CONTENTS ◄ BACK TO HIGHER-LEVEL CONTENTS